Structure, Vol. 11, 329–338, March, 2003, ©2003 Elsevier Science Ltd. All rights reserved. PII S0969-2126(03)00022-4

Structural Basis for the Antibiotic Activity of Ketolides and Azalides

Frank Schlünzen,[1,4] Jörg M. Harms,[1,4] Francois Franceschi,[3,5] Harly A.S. Hansen,[1] Heike Bartels,[1] Raz Zarivach,[1] and Ada Yonath[1,2,*]

[1]Max-Planck-Research Unit for Ribosomal Structure
22603 Hamburg
Germany

[2]Weizmann Institute
76100 Rehovot
Israel

[3]Max-Planck-Institute for Molecular Genetics
14195 Berlin
Germany

Summary

The azalide azithromycin and the ketolide ABT-773, which were derived by chemical modifications of erythromycin, exhibit elevated activity against a number of penicillin- and macrolide-resistant pathogenic bacteria. Analysis of the crystal structures of the large ribosomal subunit from *Deinococcus radiodurans* complexed with azithromycin or ABT-773 indicates that, despite differences in the number and nature of their contacts with the ribosome, both compounds exert their antimicrobial activity by blocking the protein exit tunnel. In contrast to all macrolides studied so far, two molecules of azithromycin bind simultaneously to the tunnel. The additional molecule also interacts with two proteins, L4 and L22, implicated in macrolide resistance. These studies illuminated and rationalized the enhanced activity of the drugs against specific macrolide-resistant bacteria.

Introduction

Ribosomes are large, bipartite nucleoprotein complexes responsible for the accurate translation of genetic messages. The peptide bond formation is catalyzed in the peptidyl transferase center (PTC) of the large ribosomal subunit (50S in prokaryotes). The region of the structure of the 50S subunit defining the catalytic core and the entrance to the ribosomal exit tunnel is referred to as the peptidyl transferase-associated region (PTAR), in analogy to the GTPase-associated region [1].

The integrity of the PTAR is crucial for protein biosynthesis and, hence, for the viability of all organisms, which makes the PTAR a primary target for several classes of antibiotics. Crystal structures of complexes of 50S ribosomal subunits from *Deinococcus radiodurans* [2] and *Haloarcula marismortui* [3] demonstrated that, particularly, macrolides, lincosamides, and chloramphenicol achieve their antimicrobial activity through alterations or interactions within the PTAR. Although organisms can tolerate few modifications in the PTAR without loss of viability, several mutations or posttranslational modifications, leading to antibiotic-resistant microorganisms, have been identified (reviewed in [4, 5]).

The rapid emergence of drug resistance in many pathogenic bacteria intensified the search for new antimicrobial agents, which led to the development of chemically modified macrolides, namely, the azalides [6] and ketolides [7]. Azalide antimicrobials are semisynthetic derivatives of erythromycin with a 15-membered lactone ring (Figure 1). The insertion of a methyl-substituted nitrogen in the lactone ring increases the basicity, resulting in improved acid stability and bioavailability compared with erythromycin. Ketolides are a novel class of antibiotics derived from 14-membered macrolides by substitution of the cladinose sugar by a 3-keto group (Figure 1).

In gram-negative bacteria, resistance to macrolides is frequently related to the impermeability of the cellular outer membrane because of the hydrophobic nature of macrolides [8–10]. Clinically acquired resistance to macrolides is mostly due to the production of methylases by a group of genes termed the erm genes. Azithromycin and ABT-773 were designed to overcome these obstacles and were found to yield a higher efficiency against some gram-negative respiratory pathogens, such as *Haemophilus influenzae* and enteric bacilli, including *Shigella* and *Salmonella* species [11–13]. Azithromycin has the additional advantage of prolonged tissue levels, offering short treatment regimes and improved tolerance [14]. The induction of the production of the methylases is, furthermore, suppressed for macrolides like josamycin [15, 16] and ketolides like ABT-773 [17].

We present here the crystal structures of the large ribosomal subunit of *D. radiodurans* (D50S) in complex with the azalide azithromycin and the ketolide ABT-773. The results exhibit the common features of ribosome-drug interactions among macrolides, azalides, and ketolides and elucidate the success of structural modifications of the macrolides to partially overcome antibiotic resistances. The crystallographic analyses of the binding modes of macrolides, azalides, and ketolides to the 50S ribosomal subunit provide an excellent tool for understanding how these antibiotics defeat some of the resistance mechanisms, a crucial step in the development of new drugs, based on modifications of the macrolide class of antibiotics.

Results

The crystal structures of the D50S ribosomal subunit in complex with azithromycin and ABT-773 extend the previously reported results on ribosome-macrolide complexes to two new classes of antibiotics, namely,

*Correspondence: yonath@mpgars.desy.de

[4]These authors contributed equally to this work.

[5]Present address: Rib-X Pharmaceuticals Inc., New Haven, Connecticut 06511.

Key words: ribosome; antibiotics; azithromycin; ketolides; azalides; peptidyl transferase center

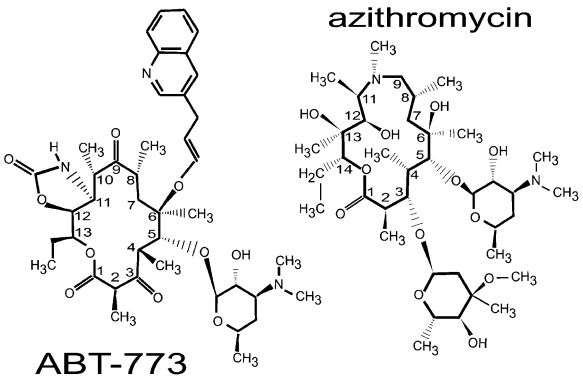

Figure 1. Chemical Structures of ABT-773 and Azithromycin
ABT-773, left; azithromycin, right.

azalides and ketolides. The crystals of the complexes were obtained by crystallization of the 50S subunit in the presence of micromolar concentrations of ABT-773 or azithromycin (see Experimental Procedures). Data have been collected for both complexes to a resolution of 3.5 Å and 3.2 Å, respectively (Table 1). The electron density maps for azithromycin and ABT-773 allowed an unambiguous determination of the binding sites of both antibiotics. The interactions of ABT-773 with specific nucleotides of the multibranched loop of domain V of 23S rRNA are rather similar to those of erythromycin, but additional contacts with domains II and IV lead to a tighter binding.

Azithromycin is, so far, the only one of these classes of antibiotics that revealed an unexpected secondary binding site. The primary site is located in a position and orientation quite similar to that observed for erythromycin or ABT-773. The second molecule was found to be in direct contact with the primary binding site, both sites blocking the path of the nascent chain. The second site directly interacts with the ribosomal protein L4 in a manner that possibly makes this site specific for *D. radiodurans*, as explained below.

The results for both azithromycin and ABT-773 are consistent with the majority of mutational and footprinting data [5, 18] (Figures 2–4), thus explaining the different modes of interactions and differences in activity against certain MLS_B-resistant phenotypes.

ABT-773

Ketolides derive their name from the insertion of a ketone bond in the C3 position and the removal of the cladinose sugar (Figure 1), which lead to a broader spectrum of activity against a number of erythromycin- or penicillin-resistant pathogens [19–21]. In addition to the C3-ketone, ABT-773 has a quinolylallyl at the C6-O position and a cyclic carbamate group at C11,12 inserted in the 14-membered lactone ring (Figure 1). The cladinose sugar was originally believed to be important for the binding of the macrolides, but our previous studies of macrolide-ribosome interactions indicated the comparatively low contribution of the cladinose moiety to the binding of the macrolides on the 50S subunit [2].

The quinolylallyl group is tethered to the macrolide skeleton through a rather flexible linker, which allows the moiety to occupy different spatial positions. The inherent flexibility is reflected by the electron density of the quinolylallyl group, which appears to be less well resolved (Figure 2A). The position of the quinolylallyl best fitting the electron density allows N3 of the quinolylallyl to form a hydrogen bond with O2′ of C803DR (U790EC) of domain II (Figures 2B and 2C). This is in agreement with biochemical experiments indicating that domain II might be involved in the binding of some of the ketolides [18, 22]. Throughout the structures of different complexes of the 50S subunit from *D. radiodurans*, we observed only a few significant variations. Among them is the loop connecting helices 32 and 35a (Figures 3 and 5D), which includes C803DR (U790EC). The base of C803DR (U790EC) appears shifted by about 2 Å toward ABT-773 compared with the native structure and by about 8 Å compared with the complex with azithromycin (see below), thus reflecting the inherent flexibility of this region.

Another region of 23S rRNA exhibiting conformational changes through the interaction with ABT-773 is the single strand composed of rRNA bases 2585–2590DR (2606–2611EC) (Figures 3 and 5D). U2588DR (U2609EC) of domain V of 23S rRNA forms a network of hydrophobic interactions with the carbamate group of ABT-773. Together with the hydrogen bond between O4 of U2588DR (U2609EC) and N2 of the carbamate group, these interactions seem to be the main contributors for the possible enhancement of the binding of ABT-773 to the ribosome, compared with other 14-membered macrolides, rendering the cladinose sugar dispensable. This is in accord with the observation that U → C2609EC mutations, which yield ABT-773- and telithromycin-resistant phenotypes, slightly increased the sensitivity to macrolides like erythromycin and azithromycin, which both lack the carbamate group [18]. As proposed [18], the enhanced potency of ABT-773 correlates with stronger interactions of the drug, with domain II of 23S rRNA through the quinolylallyl group and with domain V through the carbamate group.

Although the position of ABT-773 appears shifted compared with roxithromycin or erythromycin, it shares most of the contacts observed for these macrolides,

Table 1. Data Collection Statistics

	Resolution (Å)	Completeness	R_{sym}	I/σ(I)	R Factor	R_{free}
ABT-773	30.0–3.50	91.8%	13.1%	7.5	28.5%	31.3%
	(3.56–3.50)	(88.9%)	(35.8%)	(2.1)		
Azithromycin	30.0–3.20	86.6%	11.0%	9.0	27.9%	30.4%
	(3.25–3.20)	(83.4%)	(33.9%)	(1.9)		

Numbers in parentheses denote the highest-resolution bin.

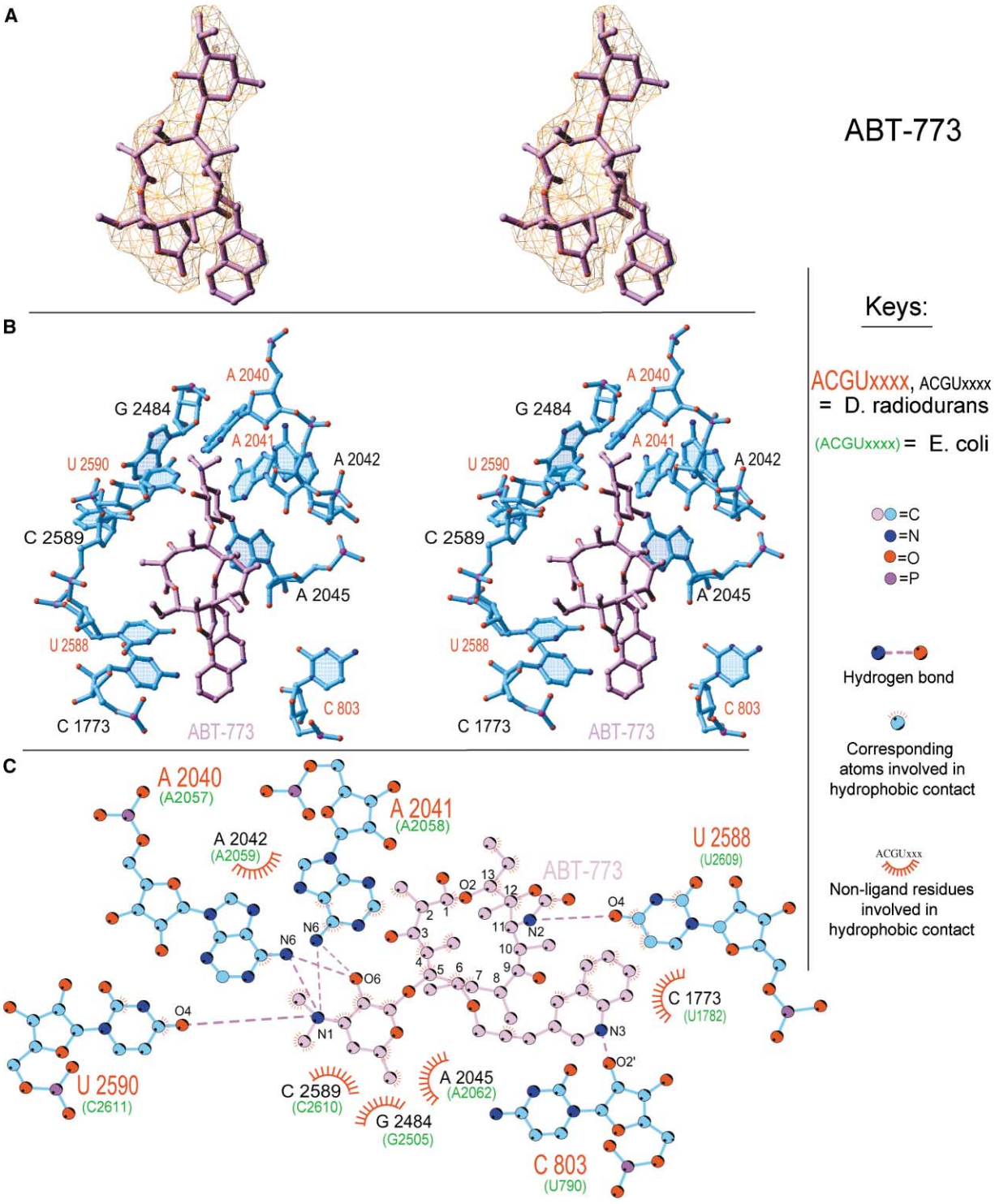

Figure 2. Electron Density and Local Environment of ABT-773

(A) Stereo views of ABT-773 together with the $2F_o - F_c$ electron density map, calculated omitting ABT-773 and contoured at 1.2 σ.

(B) Stereo view of the local environment of ABT-773. Nucleotides contributing to hydrophobic interactions are labeled in black; those contributing to hydrogen bonds are labeled in red.

(C) Two-dimensional sketch of interactions between ABT-773 and 23S rRNA. Nucleotides contributing to hydrophobic interactions are indicated; those contributing to hydrogen bonds are represented by their structures.

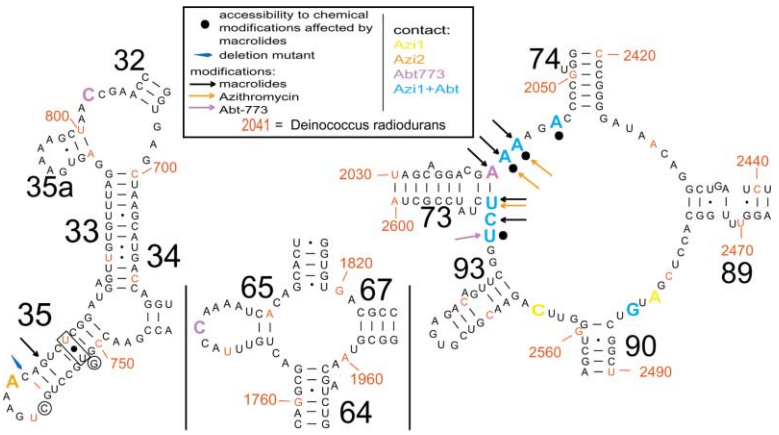

Figure 3. The Region of Domains II, IV, and V of 23S rRNA that Contributes to the Binding of ABT-773 or Azithromycin Is Shown in the Secondary Structure Diagrams

Black circles indicate changes in nucleotide accessibility affected by macrolides according to biochemical data. Modifications or mutations affecting the macrolide susceptibility or resistance are indicated by arrows. The contact sites of ABT-773 and azithromycin are indicated by large, colored letters in the diagram. The colors of the letters correspond to the colors of the ligands in Figures 2 and 4.

namely, the interactions of the desosamine with A2040DR (A2057EC) and A2041DR (A2058EC). This shift disrupts the hydrophobic contacts with A2482DR (A2503EC) but leads to additional hydrophobic contacts between the desosamine and C2589DR (C2610EC).

Interestingly, the alignment of ABT-773 with roxithromycin shows that the quinolylallyl of ABT-773 is in similar position and orientation to the oxime moiety of roxithromycin (Figures 5C and 5D); both point toward domain IV of 23S rRNA. Domain IV, which has not previously been reported to participate in the binding of ketolides, contributes to the positioning of the quinolylallyl group through hydrophobic interactions of C1773DR (U1782EC). The interactions of the quinolylallyl group with 23S rRNA seem to be completely independent of the type of the two rRNA bases involved. Mutations in either C803DR (U790EC) or C1773DR (U1782EC) are hence not expected to affect binding of ABT-773. This agrees with the observation that *E. coli*, which carries uridines in both positions (U/U), and pathogens like *Heliobacter pylori* (U/U) and *Haemophilus influenzae* (A/C) are equally susceptible to ABT-773 [23, 24].

Azithromycin

Azithromycin (CP-62,993 [9-deoxy-9A-methyl-9A-aza-9A-homoerythromycin]), the first member of the class of azalide antimicrobials, is a semisynthetic derivative of erythromycin, with a 15-membered lactone ring possessing an additional nitrogen at position C9,10 (Figure 1). On examination of the electron density of the 50S-azithromycin complex (Figure 4A), it was obvious that the mode of binding of azithromycin to the 50S ribosomal subunit from *D. radiodurans* differs significantly from the binding of all other macrolides studied so far. We found two azithromycin binding sites in the tunnel of the 50S subunit, leading to a more extended conformational change in the 23S rRNA.

The primary binding site of azithromycin (AZI-1) is located in a position and orientation similar to those of the other macrolides that we studied. In particular, the lactone ring lies in the same plane as the lactone rings of erythromycin, roxithromycin, clarithromycin, and ABT-773. Bases 2045DR (A2062EC) and U2588DR (U2609EC) contribute to the binding of AZI-1 through hydrophobic interactions. A putative Mg ion (Mg1), which is probably coordinated through water molecules, might contribute to the interactions through hydrogen bonds with the cladinose sugar and the lactone ring. Since we cannot detect water molecules at 3.5 Å resolution, the potential hydrogen bonds involving Mg1 have been omitted from Figure 4C.

Surprisingly, the nitrogen inserted into the lactone ring does not directly contribute to the binding of azithromycin. It seems, however, that this modification alters the conformation of the lactone ring sufficiently to induce novel contacts to this Mg ion and C2565DR.

Contrary to AZI-1, which interacts exclusively with domains IV and V of 23S rRNA, AZI-2 also interacts with ribosomal proteins L4 and L22 and domain II of 23S rRNA. The main source of interactions originates from hydrogen bonds between AZI-2 and the loop of L4 (Thr64 and Gly60) as well as another putative Mg ion (Figure 4).

Furthermore, AZI-2 makes a direct contact to AZI-1 through a hydrogen bond between its desosamine sugar and O1 in the lactone ring of AZI-1, which might lead to a synergetic enhancement of the binding of azithromycin. This kind of contact will probably not be possible in 14-membered macrolides, restricting the selectivity of the secondary site to 15- or 16-membered macrolides. Interestingly, the density for the lactone ring of AZI-2 is considerably better resolved than that for AZI-1. This might reflect the tightness of the AZI-2 binding pocket, which is confined by the narrowest part of the ribosomal exit tunnel, between L4 and L22, and AZI-1. The contribution of L22 originates from hydrophobic interactions between the nonconserved Arg111 and both the cladinose and the desosamine of AZI-2. The interactions between AZI-2 and L4 are more pronounced, forming hydrogen bonding interactions between Gly60 and the lactone ring as well as between the side chain of Thr64 and the cladinose (Figure 4C).

Azithromycin shares most of the interactions observed for erythromycin, namely, the contacts with A2041DR, A2042DR (A2059EC), and A2045DR (A2062EC) (Figures 3 and 4C). Only the contact with U2590DR (C2611EC) is not present in this case, which appears to be a consequence of the conformational shift of the bulged bases U2592DR (U2613EC) and A2593DR (A2614EC) of helix 73 (Figure 3). Because of the presence of AZI-2, the loop connecting helices 73 and 93 is significantly shifted. In

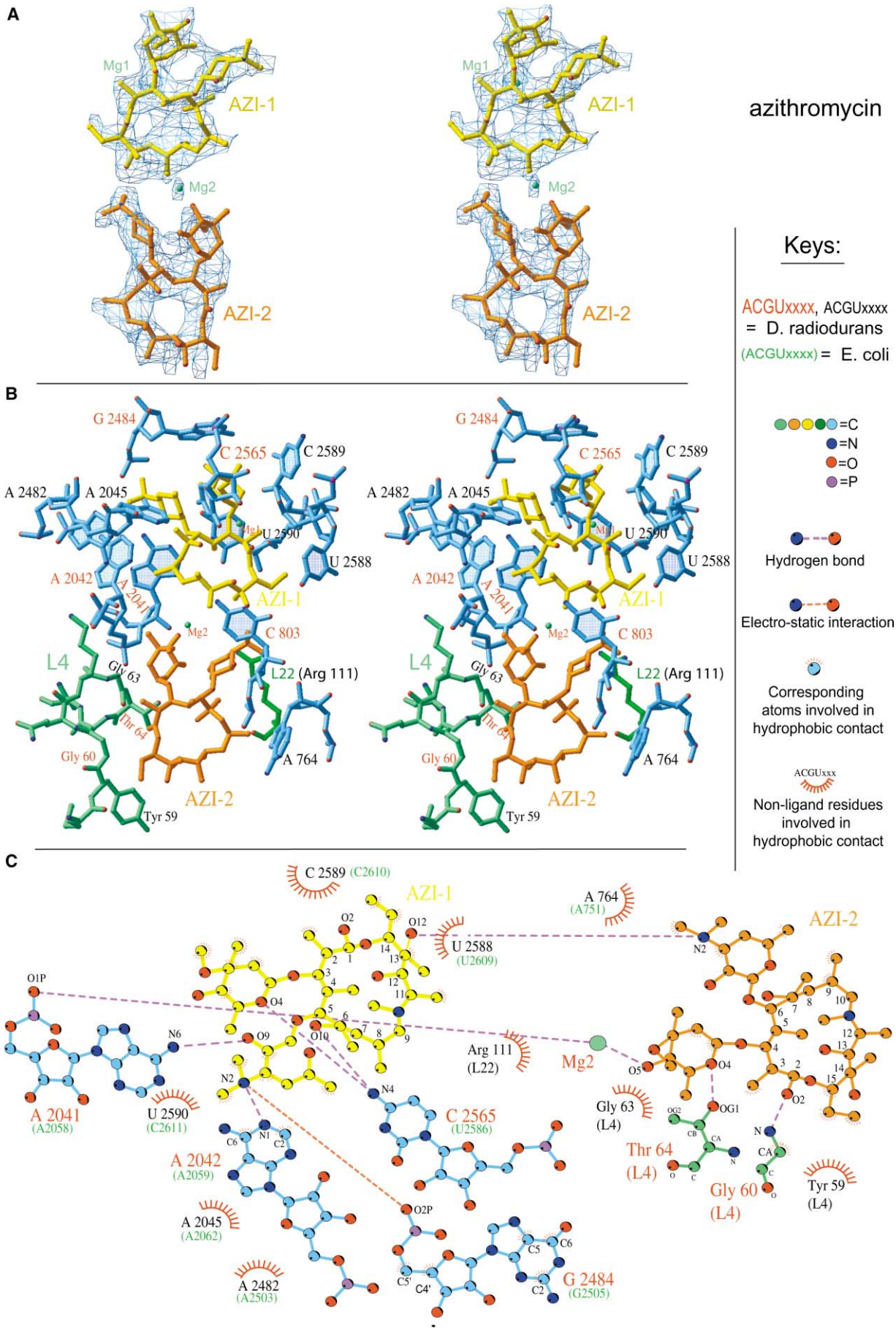
A
Mg1
AZI-1
Mg2
AZI-2
azithromycin
B
G 2484
C 2565
C 2589
A 2482
A 2045
U 2590
U 2588
A 2042
A 2041
AZI-1
Mg2
C 803
L4
Gly 63
L22 (Arg 111)
Thr 64
Gly 60
A 764
AZI-2
Tyr 59
Keys:
ACGUxxxx, ACGUxxxx
= D. radiodurans
(ACGUxxxx) = E. coli
=C
=N
=O
=P
Hydrogen bond
Electro-static interaction
Corresponding atoms involved in hydrophobic contact
ACGUxxx
Non-ligand residues involved in hydrophobic contact
C
C 2589 (C2610)
AZI-1
A 764 (A751)
AZI-2
O1P
O2
O12
U 2588 (U2609)
N2
O4
O9
O10
N6
Arg 111 (L22)
Mg2
O5
A 2041 (A2058)
U 2590 (C2611)
N4
C 2565 (U2586)
Gly 63 (L4)
Thr 64 (L4)
Gly 60 (L4)
Tyr 59 (L4)
A 2042 (A2059)
O2P
A 2045 (A2062)
A 2482 (A2503)
G 2484 (G2505)

addition to the alteration of C803DR (U790EC) mentioned above, the bases of U2588DR (U2609EC) and G2560DR (G2581EC) reveal a distinctly different orientation, G2560DR (G2581EC) being almost perpendicular to the native conformation.

Discussion

The position of ABT-773 within the PTAR appears displaced by about 3 Å compared with the position observed for the macrolides of the erythromycin class (Figure 5C) but still leads to the same inhibitory mechanism, namely, blockage of the path of the nascent chain through the 50S subunit (Figures 5A and 5B). The positional shift seems to be induced by the interactions of 23S rRNA with the different functional groups of ABT-773. This is particularly apparent through the comparison with roxithromycin (Figures 5C and 5D). Despite the difference in their positions within the 50S subunit, the oxime extension of roxithromycin and the quinolylallyl of ABT-773 align very well, supporting the importance of these functional groups for the binding of the different macrolide derivatives.

rRNA base A752EC (C765DR) was shown to be protected upon binding of ketolides carrying extensions at position C11,12 [25]. C765DR (A752EC) is in the vicinity of the binding site of ABT-773 but may partially contribute to the binding of the drug. However, exchanging C → A765DR would possibly create a direct contact between A765DR and ABT-773, consistent with biochemical data [26]. Nevertheless, it is questionable whether this interaction would further enhance the affinity of ABT-773 for 23S rRNA, since pathogens like *Heliobacter pylori* (C860, equivalent to C752EC) are equally susceptible to ketolides.

U → A754EC (G767DR) mutations in domain II have been shown to confer resistance to low levels of the ketolide HMR3647 [22]. Since neither U754EC nor C765EC has been found to be directly involved in binding of ABT-773 or any of the macrolides studied so far [2] [3], it seems that the effect of mutations of these bases on the binding of ketolides is mediated through small conformational shifts affecting the loop connecting helices H35a and H32.

Whereas the binding of ABT-773 induces—with the exception of C803DR (U790EC)—comparably small conformational changes in 23S rRNA, the two azithromycin molecules lead to more-extended shifts, particularly of the single-stranded loop connecting helices 73 and 93 (Figure 3). However, most of the contacts and the binding mode of the primary binding site remain similar to those observed for the macrolides. One remarkable exception is the additional hydrogen bond between the cladinose of AZI-1 and C2565DR (U2586EC). This hydrogen bond relies on a different orientation of the cladinose for azithromycin compared with erythromycin. Apparently, the inherent flexibility of some parts of 23S rRNA can compensate for small modifications of the antibiotics or small alterations in the binding pattern, which might explain the successful development of a large number of erythromycin derivatives with strong inhibitory activity.

The interaction of the second azithromycin site with the highly conserved loop of L4 involves Tyr59, Gly63, Thr64, and Gly60. Despite the high level of conservation, Gly60 seems to be very specific to *D. radiodurans*. Sequence alignment against all available bacterial ribosomal L4 proteins revealed no other bacterial organism with a glycine present at this position. According to the sequence alignment, 94% of the L4 sequences carry either a Lys or Arg; the remaining 6% were Pro or Ala residues. Modeling a Gly60Arg mutation into the L4 structure gave rise to a short contact of 1.5 Å between AZI-2 and L4. This indicates that, in any other bacterial 50S subunit, the binding of AZI-2 should be altered and, possibly, inhibited. Hence, the occurrence of a secondary binding site might be specific for *D. radiodurans*. This is also supported by kinetic analysis of the binding of azithromycin in *E. coli* [27], which did not reveal the pattern expected for a double binding site, though it was shown earlier that macrolides like erythromycin have the potential to bind to ribosomal proteins L5, L21, and L4 [28].

The interactions between AZI-2 and L22 exclusively involve Arg111, which is hardly conserved. It is questionable whether this interaction is crucial for the binding of AZI-2, but it would be interesting to see whether the L22 mutant described in [29] would inhibit the binding of AZI-2 or whether azithromycin still reveals an inhibitory activity on L22-mutated ribosomes of *D. radiodurans*. The conformation of the mutated L22 would certainly disrupt the hydrophobic contacts between Arg111 and AZI-2 but would not block its binding site.

While this paper was being reviewed, the structure of the 50S subunit from *H. marismortui* (H50S) in complex with azithromycin (Protein Data Bank entry 1MK1) and three other macrolides was published [3]. The position of the macrolides agrees well with our results; however, the lactone ring was found in a rather different orientation (Figure 5C). The differences in the binding pattern are also reflected by significant differences in the local RNA fold (Figure 5F). We can, as in [3], only speculate about the reason for the significant difference in the binding pattern. Despite the differences of interactions for the different macrolides, especially in the case of the two sites of azithromycin, all our data show a similar orientation of the lactone ring. It appears that the differences in the binding pattern correlate with differences

Figure 4. Electron Density and Local Environment of Azithromycin

(A) Stereo view of both azithromycin molecules together with their $2F_o - F_c$ electron density map, calculated omitting azithromycin and contoured at 1.5 σ.

(B) Stereo view of the local environment around the two azithromycin molecules. Labeling is the same as in Figure 2.

(C) Two-dimensional sketch of interactions between the two azithromycin molecules, 23S rRNA, and the ribosomal proteins L4 and L22. Nucleotides or amino acids contributing to hydrophobic interactions are indicated; those contributing to hydrogen bonds or electrostatic interactions are represented by their structures.

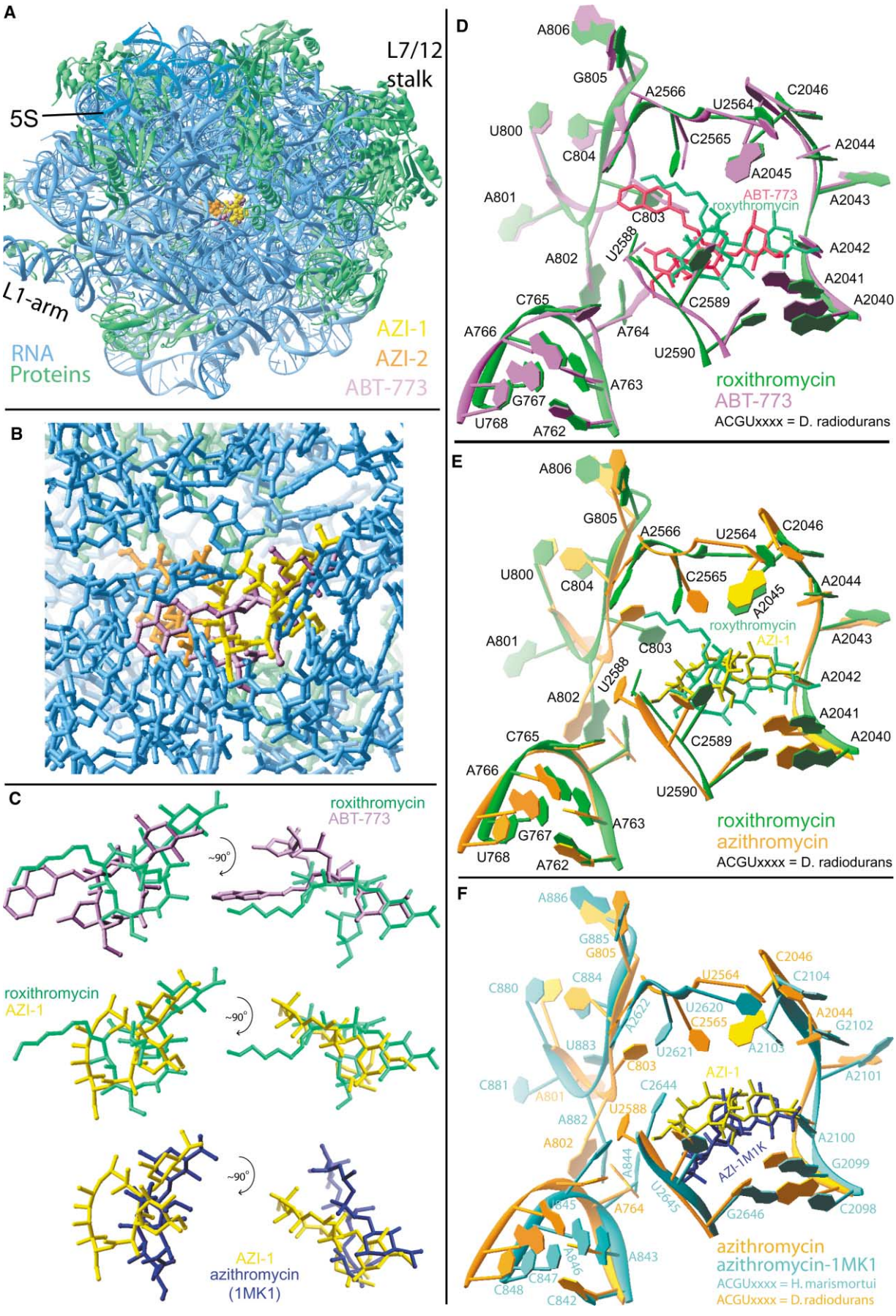
A
L7/12
stalk
5S
L1-arm
RNA
Proteins
AZI-1
AZI-2
ABT-773
B
C
roxithromycin
ABT-773
~90°
roxithromycin
AZI-1
~90°
~90°
AZI-1
azithromycin
(1MK1)
D
A806
G805
A2566
U2564
C2046
U800
C2565
A2044
C804
A2045
A801
ABT-773
roxythromycin
A2043
C803
U2588
A802
A2042
A2041
C765
C2589
A2040
A766
A764
U2590
A763
G767
U768
A762
roxithromycin
ABT-773
ACGUxxxx = D. radiodurans
E
A806
G805
A2566
U2564
C2046
U800
C804
C2565
A2044
A2045
roxythromycin
AZI-1
A801
C803
A2043
U2588
A802
A2042
A2041
C765
C2589
A2040
A766
U2590
A763
G767
U768
A762
roxithromycin
azithromycin
ACGUxxxx = D. radiodurans
F
A886
G885
G805
C2046
C884
U2564
C2104
C880
A2622
U2620
A2044
G2102
C2565
U883
U2621
A2103
C803
AZI-1
A2101
C881
C2644
A801
U2588
A882
A2100
A802
AZI-1M1K
G2099
A844
U2645
A845
A764
G2646
C2098
A846
A843
C847
C848
C842
azithromycin
azithromycin-1MK1
ACGUxxxx = H. marismortui
ACGUxxxx = D. radiodurans

in the experimental conditions and the local rRNA conformation. Our cocrystals were grown in the presence of clinically relevant concentrations of the antibiotic compounds (see Experimental Procedures), whereas extremely high-soak concentrations (1–10 mM) were used in the case of *H. marismortui* [3]. These high concentrations seem to reflect the low susceptibility of these archea to macrolides, which might be a consequence of either the extremely high salt concentrations and/or the different rRNA fold in the vicinity of the binding site. Particularly, the conformations of C2644HM (U2588DR) and U2621HM (C2565DR) are inconsistent with the azithromycin position observed in D50S, since they would have led to steric clashes and disruption of contacts between the antibiotic and 23S rRNA. Actually, the orientation of the macrolides shown in [3] yields a considerably smaller restriction of the ribosomal exit tunnel, which might suggest a comparably weaker inhibitory activity.

Biological Implications

So far, azithromycin is the only macrolide that was found to interact directly with two ribosomal proteins, namely, L4 and L22. Despite the high evolutionary conservation of the region of L4 involved in the binding of the secondary site of azithromycin, the presence of a glycine in position 60 of *D. radiodurans* is an almost singular event. It is therefore possible that the results obtained for azithromycin are partially specific for *D. radiodurans*. Studies with mutants of L4 (e.g. Gly60Arg) or antimicrobial compounds blocking the secondary binding site might reveal to what extent the secondary site alters the binding of the primary binding site of azithromycin.

The secondary AZI binding site does not appear to be responsible for the resistance mechanism against macrolides induced by mutations in L4 and L22, which were identified almost 30 years ago [30]. We did not observe a secondary binding site for any of the 14-membered macrolides bound to the D50S subunit. But, even if there were two binding sites of erythromycin in *E. coli*, the locations of the mutations are too far from the residues interacting with AZI-2 to yield a plausible resistance mechanism. Hence, our results support the idea that the resistance acquired from the mutations in L4 and L22 in *E. coli* result from conformational changes induced by these mutations [29, 31].

It has been shown that ABT-773 and azithromycin, as well as other ketolides and macrolides, inhibit the in vivo assembly of the 50S ribosomal subunit [32]. The proposal that the binding site responsible for the antimicrobial activity and the one responsible for the inhibition of 50S assembly are not identical [33] seems to agree with the structural information. Since the binding site of the macrolides is formed by nucleotides from different regions of 23S rRNA, it appears unlikely that this binding pocket will be available prior to assembly of the 50S subunit. However, the ability of antibiotics to interact with ribosomal proteins, which has been observed for macrolides, tetracycline, and evernimicin, might play an important role in the hindrance of ribosome assembly.

The crystallographic studies presented here confirm our previous results on the interactions of macrolides with the 50S ribosomal subunit and extend the findings to two novel classes of antibiotics, the ketolides and the azalides. The interactions of ABT-773 and azithromycin with D50S (Figure 3) correlate amazingly well with macrolide and ketolide resistances as well as with changes in the accessibility of the 23S rRNA to chemical modification [5]. The results emphasize the importance of the lactone ring for the proper positioning of the corresponding drug. However, the flexibility of the rRNA bases interacting with the antibiotics and, also, the flexibility of the moieties of the antibiotics involved in interactions with the ribosome can compensate, to some extent, for modifications or alterations. The differences between the binding modes of macrolides, azalides, and ketolides reveal the contributions of the chemical modifications of the macrolides, on the basis of the enhanced binding properties of these compounds as well as the resistances towards these antibiotics. Such information is of fundamental importance for the design of more potent macrolides to overcome bacterial resistance.

Experimental Procedures

Base and Amino Acid Numbering

Nucleotides named [ACGU]nnnnDR, [ACGU]nnnnEC, or [ACGU]nnnnHM are numbered according to the *D. radiodurans*, *E. coli*, or *H. marismortui* 23S rRNA sequences, respectively. Amino acids are always numbered according to the *D. radiodurans* sequences. 23S rRNA sequence alignments were based on the 2D structure diagrams obtained from http://www.rna.icmb.texas.edu [34].

50S Crystals

Crystals of the 50S ribosomal subunit were obtained as previously described [2, 35]. Cocrystallization was carried out in the presence of 7-fold excesses of azithromycin or ABT-773.

X-Ray Diffraction

Data were collected at 85 K from shock-frozen crystals with a synchrotron radiation beam at ID19 at Argonne Photon Source/Argonne National Laboratory (APS/ANL) and at ID14/2 and ID14/4 at the

Figure 5. Comparison between Several Structures of Liganded and Native 50S

(A) Overview of the 50S subunit from *D. radiodurans* (D50S) and the bound antibiotics with the axis of the ribosomal exit tunnel perpendicular to the plane.

(B) Enlarged detail of the tunnel with antibiotics. Colors are chosen as in (A).

(C) Comparison of the positions of ABT-773 and roxithromycin (top), AZI-1 and roxithromycin (middle), and AZI-1 and the corresponding molecule of azithromycin in the 50S subunit from *H. marismortui* [3] as deposited in the Protein Data Bank (1MK1) (bottom). The left column shows the antibiotics in an orientation similar to those in (A) and (B). The right column shows a view rotated by approximately 90°.

(D) The local structures of the complexes of D50S with ABT-773 and roxithromycin.

(E) The local structures of the complexes of D50S with azithromycin and roxithromycin. AZI-2 has been omitted.

(F) The local structures of the complexes of D50S and H50S with azithromycin [3]. AZI-2 has been omitted. For the sake of clarity, small parts of the local structures shown in (D) and (E) have been omitted.

European Synchrotron Radiation Facility/European Molecular Biology Laboratory (ESRF/EMBL). Data were recorded on Quantum 4 or APS-CCD detectors and processed with HKL2000 [36] and the CCP4 suite [37].

Localization and Refinement

The 3.0 Å structure of the 50S subunit (Protein Data Bank accession code 1LNR) was refined against the structure factor amplitudes of each of the two 50S-antibiotic complexes, by rigid-body refinement as implemented in CNS [38]. For the calculation of the free R factor, 7% of the data were omitted during refinement. The positions of the antibiotics were readily determined from sigma-weighted difference maps. The superior quality of the difference maps, showing the hole of the lactone ring, revealed unambiguously the position and orientation of the lactone ring. The electron density for the second binding site of azithromycin (see Figure 4A) indicated a small conformational change in the lactone ring, but these differences are considerably smaller than the average coordinate error (about 0.7 Å according to Luzzati plots). Therefore, we did not attempt to model the presumed conformational change.

Coordinates and Figures

Antibiotic compounds and corresponding ligand structures were made available by Abbott Laboratories for ABT-773 and by Pliva (Croatia) for azithromycin. Three-dimensional figures were produced with RIBBONS [39]. The 2D figures displaying the 50S-antibiotic interactions were generated with LigPlot [40].

Acknowledgments

We thank R. Albrecht, A. Bashan, W.S. Bennett, R. Berisio, C. Glotz, C. Liebe, C. Stamer, and A. Wolff for their contributions to different stages of these studies. We would like to acknowledge Abbott's and Pliva's generous gifts of the antimicrobial agents and their structures. These studies could not be performed without the excellent support by the staff of the synchrotron radiation facilities ID14-2/4 at ESRF, namely, E. Mitchell, J. McCarthy, and R. Ravelli, and the staff at the SBC beamline ID-19, namely, R. Alkire and S. Ginell. Use of the Argonne National Laboratory Structural Biology Center beamlines at the Advanced Photon Source was supported by the U.S. Department of Energy, Office of Biological and Environmental Research, under contract number W-31-109-ENG-38. Support was provided by the Max-Planck-Society, the U.S. National Institutes of Health (GM34360), the German Ministry for Science and Education (BMBF Grant 05-641EA), and the Kimmelman Center for Macromolecular Assembly at the Weizmann Institute. A.Y. holds the Helen and Martin S. Kimmel Professorial Chair.

Received: July 22, 2002
Revised: December 19, 2002
Accepted: December 19, 2002

References

1. Wimberly, B.T., Guymon, R., McCutcheon, J.P., White, S.W., and Ramakrishnan, V. (1999). A detailed view of a ribosomal active site: the structure of the L11-RNA complex. Cell *97*, 491–502.
2. Schlünzen, F., Zarivach, R., Harms, J., Bashan, A., Tocilj, A., Albrecht, R., Yonath, A., and Franceschi, F. (2001). Structural basis for the interaction of antibiotics with the peptidyl transferase centre in eubacteria. Nature *413*, 814–821.
3. Hansen, J.L., Ippolito, J.A., Ban, N., Nissen, P., Moore, P.B., and Steitz, T.A. (2002). The structures of four macrolide antibiotics bound to the large ribosomal subunit. Mol. Cell *10*, 117–128.
4. Mankin, A.S. (2001). Ribosomal antibiotics. Mol. Biol. *35*, 509–520.
5. Weisblum, B. (1998). Macrolide resistance. Drug Resist. Updat. *1*, 29–41.
6. Bright, G.M., Nagel, A.A., Bordner, J., Desai, K.A., Dibrino, J.N., Nowakowska, J., Vincent, L., Watrous, R.M., Sciavolino, F.C., and English, A.R. (1988). Synthesis, in vitro and in vivo activity of novel 9-deoxo-9a-AZA-9a-homoerythromycin A derivatives—a new class of macrolide antibiotics, the azalides. J. Antibiot. *41*, 1029–1047.
7. Agouridas, C., Denis, A., Auger, J.M., Benedetti, Y., Bonnefoy, A., Bretin, F., Chantot, J.F., Dussarat, A., Fromentin, C., D'Ambrieres, S.G., et al. (1998). Synthesis and antibacterial activity of ketolides (6-O-methyl-3-oxoerythromycin derivatives): a new class of antibacterials highly potent against macrolide-resistant and -susceptible respiratory pathogens. J. Med. Chem. *41*, 4080–4100.
8. Montenez, J.P., Van Bambeke, F., Piret, J., Brasseur, R., Tulkens, P.M., and Mingeot-Leclercq, M.P. (1999). Interactions of macrolide antibiotics (erythromycin A, roxithromycin, erythromycylamine [dirithromycin], and azithromycin) with phospholipids: computer-aided conformational analysis and studies on acellular and cell culture models. Toxicol. Appl. Pharmacol. *156*, 129–140.
9. Savage, P.B. (2001). Multidrug-resistant bacteria: overcoming antibiotic permeability barriers of gram-negative bacteria. Ann. Med. *33*, 167–171.
10. Vaara, M. (1993). Outer-membrane permeability barrier to azithromycin, clarithromycin, and roxithromycin in gram-negative enteric bacteria. Antimicrob. Agents Chemother. *37*, 354–356.
11. Rakita, R.M., Jacquespalaz, K., and Murray, B.E. (1994). Intracellular activity of azithromycin against bacterial enteric pathogens. Antimicrob. Agents Chemother. *38*, 1915–1921.
12. Gur, D., Kayaokay, Y., Hascelik, G., and Akalin, H.E. (1993). In vitro activity of azithromycin against trimethoprim-sulfamethoxazole resistant Salmonella enteritidis and Shigella spp. J. Chemother. Suppl. *5*, 151–152.
13. Gordillo, M.E., Singh, K.V., and Murray, B.E. (1993). In vitro activity of azithromycin against bacterial enteric pathogens. Antimicrob. Agents Chemother. *37*, 1203–1205.
14. Alvarez-Elcoro, S., and Enzler, M.J. (1999). The macrolides: erythromycin, clarithromycin, and azithromycin. Mayo Clin. Proc. *74*, 613–634.
15. Giovanetti, E., Montanari, M.P., Mingoia, M., and Varaldo, P.E. (1999). Phenotypes and genotypes of erythromycin-resistant Streptococcus pyogenes strains in Italy and heterogeneity of inducibly resistant strains. Antimicrob. Agents Chemother. *43*, 1935–1940.
16. Hamiltonmiller, J.M.T. (1992). In vitro activities of 14-membered, 15-membered and 16-membered macrolides against gram-positive cocci. J. Antimicrob. Chemother. *29*, 141–147.
17. Bonnefoy, A., Girard, A.M., Agouridas, C., and Chantot, J.F. (1997). Ketolides lack inducibility properties of MLS(B) resistance phenotype. J. Antimicrob. Chemother. *40*, 85–90.
18. Garza-Ramos, G., Xiong, L.Q., Zhong, P., and Mankin, A. (2001). Binding site of macrolide antibiotics on the ribosome: new resistance mutation identifies a specific interaction of ketolides with rRNA. J. Bacteriol. *183*, 6898–6907.
19. Davies, T.A., Ednie, L.M., Hoellman, D.M., Pankuch, G.A., Jacobs, M.R., and Appelbaum, P.C. (2000). Antipneumococcal activity of ABT-773 compared to those of 10 other agents. Antimicrob. Agents Chemother. *44*, 1894–1899.
20. Rosato, A., Vicarini, H., Bonnefoy, A., Chantot, J.F., and Leclercq, R. (1998). A new ketolide, HMR 3004, active against streptococci inducibly resistant to erythromycin. Antimicrob. Agents Chemother. *42*, 1392–1396.
21. Nagai, K., Davies, T.A., Ednie, L.M., Bryskier, A., Palavecino, E., Jacobs, M.R., and Appelbaum, P.C. (2001). Activities of a new fluoroketolide, HMR 3787, and its (des)-fluor derivative RU 64399 compared to those of telithromycin, erythromycin A, azithromycin, clarithromycin, and clindamycin against macrolide-susceptible or -resistant Streptococcus pneumoniae and S-pyogenes. Antimicrob. Agents Chemother. *45*, 3242–3245.
22. Xiong, L.Q., Shah, S., Mauvais, P., and Mankin, A.S. (1999). A ketolide resistance mutation in domain II of 23S rRNA reveals the proximity of hairpin 35 to the peptidyl transferase centre. Mol. Microbiol. *31*, 633–639.
23. Andrews, J.M., Weller, T.M.A., Ashby, J.P., Walker, R.M., and Wise, R. (2000). The in vitro activity of ABT773, a new ketolide antimicrobial agent. J. Antimicrob. Chemother. *46*, 1017–1022.
24. Credito, K.L., Lin, G.R., Pankuch, G.A., Bajaksouzian, S., Ja-

cobs, M.R., and Appelbaum, P.C. (2001). Susceptibilities of Haemophilus influenzae and Moraxella catarrhalis to ABT-773 compared to their susceptibilities to 11 other agents. Antimicrob. Agents Chemother. *45*, 67–72.

25. Hansen, L.H., Mauvais, P., and Douthwaite, S. (1999). The macrolide-ketolide antibiotic binding site is formed by structures in domains II and V of 23S ribosomal RNA. Mol. Microbiol. *31*, 623–631.
26. Douthwaite, S., Hansen, L.H., and Mauvais, P. (2000). Macrolide-ketolide inhibition of MLS-resistant ribosomes is improved by alternative drug interaction with domain II of 23S rRNA. Mol. Microbiol. *36*, 183–192.
27. Dinos, G.P., Michelinaki, M., and Kalpaxis, D.L. (2001). Insights into the mechanism of azithromycin interaction with an Escherichia coli functional ribosomal complex. Mol. Pharmacol. *59*, 1441–1445.
28. Suryanarayana, T. (1983). Identification by affinity-chromatography of Escherichia coli ribosomal proteins that bind erythromycin and chloramphenicol. Biochem. Int. *7*, 719–725.
29. Davydova, N., Streltsov, V., Wilce, M., Liljas, A., and Garber, M. (2002). L22 ribosomal protein and effect of its mutation on ribosome resistance to erythromycin. J. Mol. Biol. *322*, 635.
30. Wittmann, H.G., Stoffler, G., Apirion, D., Rosen, L., Tanaka, K., Tamaki, M., Takata, R., Dekio, S., Otaka, E., and Osawa, S. (1973). Biochemical and genetic studies on 2 different types of erythromycin resistant mutants of Escherichia coli with altered ribosomal proteins. Mol. Gen. Genet. *127*, 175–189.
31. Gabashvili, I.S., Gregory, S.T., Valle, M., Grassucci, R., Worbs, M., Wahl, M.C., Dahlberg, A.E., and Frank, J. (2001). The polypeptide tunnel system in the ribosome and its gating in erythromycin resistance mutants of L4 and L22. Mol. Cell *8*, 181–188.
32. Champney, W.S., and Burdine, R. (1998). Macrolide antibiotic inhibition of translation and 50S ribosomal subunit assembly in methicillin-resistant Staphylococcus aureus cells. Microb. Drug Resist. *4*, 169–174.
33. Champney, W.S., Tober, C.L., and Burdine, R. (1998). A comparison of the inhibition of translation and 50S ribosomal subunit formation in Staphylococcus aureus cells by nine different macrolide antibiotics. Curr. Microbiol. *37*, 412–417.
34. Cannone, J.J., Subramanian, S., Schnare, M.N., Collett, J.R., D'Souza, L.M., Du, Y., Feng, B., Lin, N., Madabusi, L.V., Müller, K.M., et al. (2002). The comparative RNA Web (CRW) site: an online database of comparative sequence and structure information for ribosomal, intron, and other RNAs. BMC Bioinformatics *3*, 2.
35. Harms, J., Schluenzen, F., Zarivach, R., Bashan, A., Gat, S., Agmon, I., Bartels, H., Franceschi, F., and Yonath, A. (2001). High resolution structure of the large ribosomal subunit from a mesophilic eubacterium. Cell *107*, 679–688.
36. Otwinowski, Z., and Minor, W. (1997). Processing of X-ray diffraction data collected in oscillation mode. Methods Enzymol. *276*, 307–326.
37. Bailey, S. (1994). The CCP4 suite: programs for protein crystallography. Acta Crystallogr. D Biol. Crystallogr. *50*, 760–763.
38. Brunger, A.T., Adams, P.D., Clore, G.M., DeLano, W.L., Gros, P., Grosse-Kunstleve, R.W., Jiang, J.S., Kuszewski, J., Nilges, M., Pannu, N.S., et al. (1998). Crystallography and NMR system: a new software suite for macromolecular structure determination. Acta Crystallogr. D Biol. Crystallogr. *54*, 905–921.
39. Carson, M. (1997). Ribbons. Methods Enzymol. *277*, 493–505.
40. Wallace, A.C., Laskowski, R.A., and Thornton, J.M. (1995). Ligplot—a program to generate schematic diagrams of protein ligand interactions. Protein Eng. *8*, 127–134.

Accession Numbers

Final coordinates have been deposited in the Protein Data Bank under accession numbers 1NWX and 1NWY.